Probing the Bond Order Wave Phase Transitions of the Ionic Hubbard Model by Superlattice Modulation Spectroscopy

Karla Loida,[1] Jean-Sébastien Bernier,[1] Roberta Citro,[2] Edmond Orignac,[3] and Corinna Kollath[1]
[1]HISKP, University of Bonn, Nussallee 14-16, 53115 Bonn, Germany
[2]Dipartimento di Fisica "E.R. Caianiello" and CNR-SPIN, Università degli Studi di Salerno, Via Giovanni Paolo II 132, I-84084 Fisciano (Sa), Italy
[3]Université de Lyon, École Normale Supérieure de Lyon, Université Claude Bernard, CNRS, Laboratoire de Physique, F-69342 Lyon, France
(Received 3 June 2017; published 6 December 2017)

An exotic phase, the bond order wave, characterized by the spontaneous dimerization of the hopping, has been predicted to exist sandwiched between the band and Mott insulators in systems described by the ionic Hubbard model. Despite growing theoretical evidence, this phase still evades experimental detection. Given the recent realization of the ionic Hubbard model in ultracold atomic gases, we propose here to detect the bond order wave using superlattice modulation spectroscopy. We demonstrate, with the help of time-dependent density-matrix renormalization group and bosonization, that this spectroscopic approach reveals characteristics of both the Ising and Kosterlitz-Thouless transitions signaling the presence of the bond order wave phase. This scheme also provides insights into the excitation spectra of both the band and Mott insulators.

DOI: 10.1103/PhysRevLett.119.230403

In solid state materials, the combination of strong interactions, quantum fluctuations, and finely tuned energy scales gives rise to rich physics. For example, in a large class of materials including transition metal oxides [1], organics [2] and iridates [3], the presence of strong repulsion between fermions leads to the formation of Mott insulating states. Inducing charge fluctuations around these Mott insulators, e.g., by doping, reveals intricate phase diagrams highlighting the presence of multiple competing orders. Perhaps one of the best known examples is the emergence of d-wave superconductivity in high-temperature cuprates at the interface between antiferromagnetic and Fermi liquid phases [4].

Complex states also arise near phase transitions when competing insulating effects are present. In the neighborhood of such transitions, where the strength of the insulating terms is comparable, the effect of smaller terms, such as the kinetic energy, leads to the emergence of metallic phases or exotic correlations. For example, at the interface between the Mott and band insulators, such a competition is believed to play an important role in the ionic to neutral transitions in organic charge-transfer solids [5,6] and at ferroelectric transitions in perovskites [7]. The ionic Hubbard model, which gained prominence over the last decade, was first developed to explain the physics near these transitions. In this model, the on-site Hubbard repulsion and staggered potential terms induce insulating behavior when taken separately, but when taken together they can compete and give rise to a region of increased charge fluctuations. This region is of great interest as this competition leads to the emergence of the bond order wave phase signaled by a spontaneous dimerization of the hopping.

The ionic Hubbard model is given by

$$\hat{H}_0 = -J\sum_{j=1,\sigma}^{L-1}(c_{j\sigma}^{\dagger}c_{j+1\sigma} + \text{H.c.}) + U\sum_{j=1}^{L} n_{j\uparrow}n_{j\downarrow} + \frac{\Delta}{2}\sum_{j=1,\sigma}^{L}(-1)^j n_{j\sigma}.$$

Here $c_{j,\sigma}^{(\dagger)}$ are the fermionic annihilation (creation) operators and $n_{j,\sigma}$ is the particle number operator on site j with spin $\sigma = \{\uparrow, \downarrow\}$. The amplitude J is the hopping matrix element, U the repulsive on-site interaction strength, Δ an energy offset between neighboring sites (leading to a staggered potential), and L the number of sites. In one dimension, this model has been the subject of many studies using a variety of techniques including bozonization, density renormalization group, exact diagonalization, and quantum Monte Carlo methods [8–19]. A smaller number of studies have also focused on the excitations of the ionic Hubbard model [20–24]. Despite initial controversy, theoretical investigations point to the existence, at half filling, of a bond order wave phase occuring around $U \sim \Delta$, characterized by the spontaneous dimerization of the hopping, i.e., the order parameter $B = |\langle\hat{B}\rangle|$, where $\hat{B} = \sum_{j=1,\sigma}^{L-1}(-1)^j(c_{j\sigma}^{\dagger}c_{j+1\sigma} + \text{H.c.})$. The bond order wave spontaneously breaks site-inversion symmetry, and, in the limit of infinite system size, the state is twofold degenerate with restored bond-inversion symmetry on either even or odd bonds. The bond order wave phase possesses finite charge and spin gaps and is separated, on the one side, from a band insulating state by an Ising quantum phase transition and, on the other side, from a Mott insulator

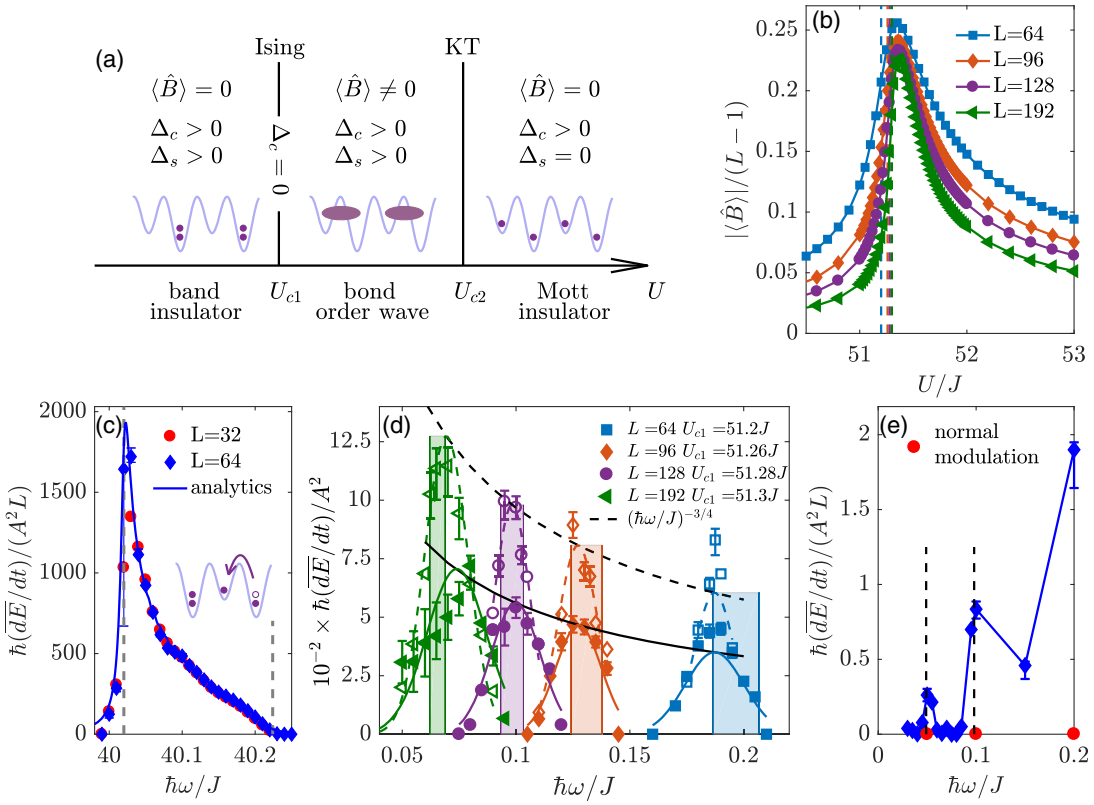

FIG. 1. (a) Phase diagram of the 1D ionic Hubbard model as a function of U for fixed Δ and J. Δ_c and Δ_s are the charge and spin gaps. (b) The bond order parameter $|\langle\hat{B}\rangle|$ at fixed $\Delta = 50J$ for different system sizes calculated from DMRG keeping up to 400 states. The dashed vertical lines mark the position of the maximum of the derivative located at $U_{c1} \sim 51.2J, 51.26J, 51.28J, 51.3J$ for system sizes $L = 64, 96, 128, 192$, respectively. (c)–(e) Energy absorption rate for different regions of the phase diagram at fixed $\Delta = 50J$: (c) Deep in the band insulator for $U = 10J$, $A = 0.001J$, dashed vertical lines mark the width of the band of excitations; (d) At the Ising critical point for different system sizes and amplitudes $A = 0.001J$ (filled symbols) and $A = 0.0005J$ (open symbols). The Gaussian fits (solid and dashed lines) are guides to the eye, where the maxima are fixed to $\lambda(\hbar\omega/J)^{-3/4}$ with λ chosen to agree with the $L = 128$ peaks; (e) In the bond order wave phase near the KT transition for $L = 64$, $U = 52J$, and $A = 0.005J$. Vertical dashed lines indicate multiples of the spin gap.

by a Kosterlitz-Thouless (KT) transition [Fig. 1(a)]. Despite strong theoretical evidence, the bond order wave has yet to be experimentally detected.

Ultracold fermionic gases provide an appealing novel avenue to detect this state. The ionic Hubbard model was recently realized using fermions loaded into an optical superlattice potential [25,26]. Furthermore, over the last decade, powerful detection techniques were developed to probe the intricate physics of quantum gases. For instance, characteristic excitations of correlated systems can be probed using various spectroscopic techniques such as radio frequency, Raman, Bragg, and lattice modulation spectroscopy [26–43].

However, detecting the bond order wave and characterizing the nature of the neighboring phase transitions remains to be done. One important challenge is to identify a suitable observable to detect the bond order wave. Directly measuring the order parameter is difficult as this would require a measurement of the staggered kinetic energy. Alternatively, a promising approach to characterize the neighboring phase transitions is to study the response of the system to a perturbation. This requires the development of a technique which, in contrast to available probes, couples directly to the order parameter. We demonstrate here, using time-dependent matrix renormalization group (t-DMRG) [44–46] and bosonization techniques [47–49], that *superlattice* amplitude modulation spectroscopy reveals features of both the Ising and KT transitions in one-dimensional systems signaling the presence of the bond order wave phase. This modulation also provides insights into the excitation spectra of both the band and Mott insulators, the two phases bordering the bond order wave. On the band insulating side, near the Ising transition, one can follow the closing of the charge excitation gap. On the bond order side of the KT transition, one can study the closing of the spin gap which then remains closed in the Mott insulator. The proposed detection method relies on inducing a small time-periodic modulation of the superlattice potential described by the perturbation $\hat{H}_{\text{pert}} = A\sin(\omega t)\hat{B}$, with A the strength and ω the frequency of the modulation directly coupling to the

order parameter. By contrast with standard lattice amplitude modulation, here the lattice is modulated in a dimerized fashion. Experimentally, such a perturbation is achievable by time-periodically tuning the phase between the two laser waves generating the optical superlattice. The parameters can be chosen such that the phase modulation translates into an alternating modulation of the lattice height while the bottom offsets stay approximately constant which is equivalent to a dimerized modulation of the hopping amplitude. The number of excitations created through the modulation is then assessed by monitoring the absorbed energy.

Using t-DMRG, we determine the evolution of the full system $\hat{H}_0 + \hat{H}_{\text{pert}}$, with open boundary conditions, and compute the energy of the system as a function of time. Typically, the energy shows a quadratic rise at initial times before entering a linear regime and then saturates at later times. We extract the slope of the linear energy increase, a quantity we identify as the energy absorption rate [50]. For the time evolution using t-DMRG we typically keep 120 states (except at the Ising critical point where we keep 160). The error analysis is performed by increasing the matrix dimension to 160 states (and 240 at the Ising critical point). The time step of the Trotter-Suzuki time evolution is set to $J\Delta t = 0.001\hbar$ and we use $J\Delta t = 0.0005\hbar$ to conduct the error analysis. The error bars provided in the figures represent the maximal uncertainties due to the matrix dimension, the time step, and the fit error (as the fit range has been varied).

In the limit of sufficiently weak modulation strength, where linear response theory applies, the energy absorption rate is related to the dynamic susceptibility as $\overline{dE}/dt \sim \omega A^2 \mathrm{Im}\chi_{\hat{B}\hat{B}^\dagger}(\omega)$. Here the dynamic susceptibility $\chi_{\hat{B}\hat{B}^\dagger}(\omega)$ is determined by the Fourier transform of the retarded correlation function $\chi_{\hat{B}\hat{B}^\dagger}(t) = -i\theta(t)\langle[\hat{B}(t), \hat{B}^\dagger(0)]\rangle_0$, where $\langle\cdot\rangle_0$ denotes the expectation value in the ground state.

We first consider the energy absorption rate at the Ising critical point U_{c1}. Within bosonization, $\hat{B}$ is proportional to the Ising order parameter in the vicinity of the Ising transition [8,9]. At the Ising quantum critical point, the scaling dimension of the order parameter is $1/8$. Estimating its dynamic susceptibility at criticality by a scaling argument, we find the absorbed power to diverge as $L\omega^{-3/4}$ in the thermodynamic limit as the modulation frequency decreases to zero signaling the Ising transition. At frequencies lower than the spin gap, the charge fluctuations dominate causing the divergence. One should note that normal lattice modulation fails to detect the existence of the Ising phase transition. In this case, the energy absorption rate does not present a divergence at the Ising transition as this latter modulation scheme does not couple to the bond order wave.

The form of the divergence is affected by the system size. In a finite system, we find [50]

$$\mathrm{Im}\chi_{\hat{B}\hat{B}^\dagger}(\omega) \sim L^{\frac{7}{4}} \sum_{n=0}^{\infty} \left(\frac{\Gamma(n+1/8)}{\Gamma(n+1)}\right)^2 \delta[\hbar(\omega - \Omega(n))],$$

with $\hbar\Omega(n) = 4\pi\frac{\hbar u_c}{aL}(n + \frac{1}{16})$, where a is the lattice spacing and u_c the sound velocity of the low energy charge excitations. Thus, for a finite system, the divergence will be signaled by the presence of a series of peaks occuring at $\hbar\Omega(n)$ with spectral weight scaling as $\omega^{-3/4}$.

In order to test these low energy predictions, we time evolve systems of different sizes at the Ising critical point for a range of modulation frequencies and extract the energy absorption rates. At low energies ($\hbar\omega/J < 0.15$), both our numerical results and our predictions from bosonization are in good agreement: the peaks height follows well the $(\hbar\omega/J)^{-3/4}$ divergence. To identify values of U/J near the Ising critical point $(U/J)_{c1}$, we find for each system size the location of the maximum of the derivative of the order parameter, $\partial|\langle\hat{B}\rangle|/\partial U$ [Fig. 1(b)]. Analyzing the energy absorption rate at these values, we then identify the $n = 1$ peak [64]. We estimate the peak position by fitting to the t-DMRG data, for the system of size $L = 128$ and modulation amplitude $A = 0.0005J$, a Gaussian approximating the δ function with a finite broadening. We find $\hbar\omega_{\text{peak}}/J \approx 0.098 \pm 0.005$. From this we extract the sound velocity of excitations $(\hbar u_c/aJ) \approx 0.94 \pm 0.05$, a typical value for lattice systems [65].

The agreement between the peaks predicted from bosonization using this value of u_c [indicated in Fig. 1(d) by shaded regions] and the t-DMRG ones is good. We attribute the disagreement in the peak position and height for $L = 64$ to the breakdown of bosonization in the energy range where the corresponding $n = 1$ peak appears. While the asymmetry of the $n = 1$ peak at $L = 192$ and $A = 0.001J$ is due to saturation effects in the numerics. Slightly above and slightly below Ising criticality the charge gap reopens [50].

The approach to the Ising phase transition is also detected from the signal obtained on the band insulating side as one can follow the linear closing of the charge gap as the system approaches the critical point. Deep within the band insulator, shown in Fig. 1(c), the absorption peak is located approximately at $\hbar\omega \sim (\Delta - U)$, corresponding to the naive expectation of breaking a doublon on a low energy site and of transferring one particle to the neighboring high energy site. The peak is very sharp and its width scales approximately as $J^2/(\Delta - U)$ as the excitation can travel through the lattice via virtual processes. A strong rise occurs at its left boundary corresponding to a divergence at the lower excitation band edge as also seen in the noninteracting model. The location, width, and shape of the peak deep in the band insulator [see solid line in Fig. 1(c)] is understood within an effective model using a Schrieffer-Wolff transformation for the excited states [66]. When approaching the Ising transition by increasing U, the peak broadens and shifts towards smaller energies. The position of the peak maximum as a function of U is shown in Fig. 2, thus confirming that the charge gap closes when approaching the Ising phase transition.

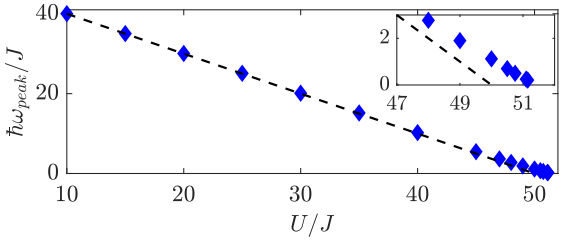

FIG. 2. The position of the maximum of the absorption peak $\hbar\omega_{\mathrm{peak}}$ corresponds approximately to the charge gap on the band-insulating side ($\Delta > U$) at fixed $\Delta = 50J$ and $L = 64$. Inset: close to the transition the deviation from the naive expectation $\Delta - U$ (dashed line) increases.

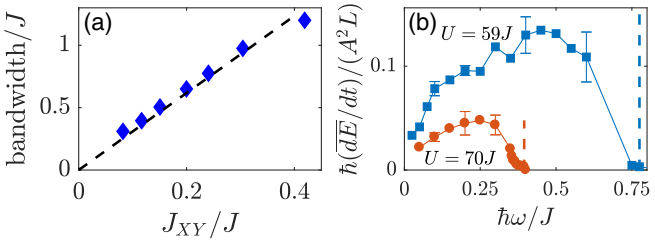

FIG. 3. (a) Width of the low energy band of spin excitations in the Mott insulator, extracted from the energy absorption rate, as a function of the effective spin coupling J_{XY} for $\Delta < U$ at fixed $\Delta = 50J$ and $L = 64$, $A = 0.005J$. The dashed line is a linear fit to the data. (b) Energy absorption rate as a function of $\hbar\omega$ ($\Delta = 50J$, $L = 64$, $A = 0.005J$).

By comparison to the Ising transition, the location of the KT quantum critical point is harder to pinpoint in finite size systems as the bond order wave order parameter falls off very slowly; see Fig. 1(b). Nevertheless, to the left of the KT transition on the bond order wave side, bosonization predicts a gapped response followed by a sharp increase of the energy absorption rate at twice the minimum energy (mass) of a soliton, μ, corresponding to the creation of a soliton-antisoliton pair [50],

$$\mathrm{Im}\chi_{\hat{B}\hat{B}^\dagger}(\omega) \sim \frac{1}{J}\sqrt{\left(\frac{\hbar\omega}{2\mu}\right)^2 - 1}.$$

In the spontaneous dimerized phase, singlets form either on even or odd bonds, giving rise to a doubly degenerate ground state and solitons are interpreted as domain walls between the two ground states. The operator $\hat{B}$ is SU(2) invariant, and can only induce transitions from the singlet ground state to excited states within the same spin sector. The lowest available state is a pair of domain walls (solitons) of opposite spins giving a threshold at twice the soliton mass [67].

We test this prediction near this second phase boundary at $U = 52J$. As shown in Fig. 1(e), we observe sharp rises of the absorption rate at multiples of the spin gap value. The spin gap is obtained from static DMRG calculations in different $S_z = N_\uparrow - N_\downarrow$ sectors, $\Delta_s = E_0(N = N_\uparrow + N_\downarrow = L, S_z = 2) - E_0(N = N_\uparrow + N_\downarrow = L, S_z = 0)$. For $U = 52J$ we find $\Delta_s \approx 0.049J$ for $L = 64$ converged in the matrix dimension. Note, that the normal lattice modulation does not couple to the soliton-antisoliton excitation. Approaching the KT transition from the bond order wave side, the soliton mass becomes smaller and smaller until at the transition the gap closes and a low energy feature, associated with spin excitations, arises on the Mott-insulating side. Hence, superlattice modulation succeeds in signaling the proximity of the KT quantum critical point. In the Mott insulating phase, the averaged energy absorption rate is predicted by bosonization to be constant at low modulation frequencies in the infinite size limit. In fact, in a finite system we expect equal weight peaks, which blend into a constant spectrum when $L \to \infty$. This spectrum, whose amplitude decreases with increasing U, is bounded by the low energy cutoff. Our numerical results for the case of the Mott insulator show at low energies a broad excitation spectrum [see Fig. 3(b)]. We also find that the width and height of the spectrum decrease with increasing U. These different features corroborate the predictions from bosonization. Additionally, due to the dominant role played by the spin degrees of freedom, for $J \ll U - \Delta$, the ionic Hubbard model can be mapped at low energies onto an isotropic Heisenberg chain with exchange interaction $J_{XY} = J_Z = (4J^2/U)[1/(1 - (\Delta/U)^2)]$ [6]. As seen in Fig. 3, the width of the spectrum increases linearly with the strength of the Heisenberg exchange interaction confirming the spin nature of this excitation spectrum. Substructures in the spectrum might arise at longer time scales as revealed in [31] for the homogeneous Hubbard model.

In summary, we demonstrated that superlattice modulation spectroscopy can be used to detect features of both the Ising and KT transitions signaling the presence of the bond order wave phase. This approach would provide a first experimental glimpse into a phase that has evaded detection in the solid state context and highlights the versatility of spectroscopic methods.

To facilitate the detection of these various features, care should be taken to choose experimental parameters for which the bond order wave is robust and has a finite (preferably large) extension, a feature increasing with the energy offset Δ [16]. While the band insulator and bond order wave are both robust due to their gapped spectrum, at Ising criticality and in the Mott insulator, the gap closes. Therefore, conducting the experiment at a temperature below $\sim J^2/(\Delta + U)$, the lowest energy scale for charge and spin fluctuations, is desirable. This is a similar scale as for the antiferromagnetic phase, a situation where relevant correlations were recently experimentally observed [68–70]. The band insulator and the bond order wave state are also robust to a weak trapping potential; however, at the Ising critical point a homogeneous potential [71–73] would be advantageous to unambigiously identify the critical scaling behavior.

We thank T. Giamarchi and A. Sheikhan for insightful discussions. We acknowledge financial support of the DFG (SFB 1238 project C05 and TR 185 project B4), ERC Phonton (648166).

[1] M. Imada, A. Fujimori, and Y. Tokura, Rev. Mod. Phys. **70**, 1039 (1998).
[2] B. J. Powell and R. H. McKenzie, Rep. Prog. Phys. **74**, 056501 (2011).
[3] W. Witczak-Krempa, G. Chen, Y. B. Kim, and L. Balents, Annu. Rev. Condens. Matter Phys. **5**, 57 (2014).
[4] J. G. Bednorz and K. A. Mueller, Z. Phys. B **64**, 189 (1986).
[5] J. B. Torrance, A. Girlando, J. J. Mayerle, J. I. Crowley, V. Y. Lee, P. Batail, and S. J. LaPlaca, Phys. Rev. Lett. **47**, 1747 (1981).
[6] N. Nagaosa and J. Takimoto, J. Phys. Soc. Jpn. **55**, 2735 (1986).
[7] T. Egami, S. Ishihara, and M. Tachiki, Science **261**, 1307 (1993).
[8] M. Fabrizio, A. O. Gogolin, and A. A. Nersesyan, Phys. Rev. Lett. **83**, 2014 (1999).
[9] M. Fabrizio, A. Gogolin, and A. Nersesyan, Nucl. Phys. **B580**, 647 (2000).
[10] N. Gidopoulos, S. Sorella, and E. Tosatti, Eur. Phys. J. B **14**, 217 (2000).
[11] T. Wilkens and R. M. Martin, Phys. Rev. B **63**, 235108 (2001).
[12] M. E. Torio, A. A. Aligia, and H. A. Ceccatto, Phys. Rev. B **64**, 121105 (2001).
[13] A. P. Kampf, M. Sekania, G. I. Japaridze, and P. Brune, J. Phys. Condens. Matter **15**, 5895 (2003).
[14] Y. Z. Zhang, C. Q. Wu, and H. Q. Lin, Phys. Rev. B **67**, 205109 (2003).
[15] C. D. Batista and A. A. Aligia, Phys. Rev. Lett. **92**, 246405 (2004).
[16] S. R. Manmana, V. Meden, R. M. Noack, and K. Schönhammer, Phys. Rev. B **70**, 155115 (2004).
[17] H. Otsuka and M. Nakamura, Phys. Rev. B **71**, 155105 (2005).
[18] O. Legeza, K. Buchta, and J. Sólyom, Phys. Rev. B **73**, 165124 (2006).
[19] L. Tincani, R. M. Noack, and D. Baeriswyl, Phys. Rev. B **79**, 165109 (2009).
[20] A. A. Aligia and C. D. Batista, Phys. Rev. B **71**, 125110 (2005).
[21] M. Hafez and S. A. Jafari, Eur. Phys. J. B **78**, 323 (2010).
[22] A. Go and G. S. Jeon, Phys. Rev. B **84**, 195102 (2011).
[23] M. Hafez-Torbati, N. A. Drescher, and G. S. Uhrig, Phys. Rev. B **89**, 245126 (2014).
[24] M. Hafez-Torbati, N. A. Drescher, and G. S. Uhrig, Eur. Phys. J. B **88**, 36 (2015).
[25] L. Tarruell, D. Greif, T. Uehlinger, G. Jotzu, and T. Esslinger, Nature (London) **483**, 302 (2012).
[26] M. Messer, R. Desbuquois, T. Uehlinger, G. Jotzu, S. Huber, D. Greif, and T. Esslinger, Phys. Rev. Lett. **115**, 115303 (2015).
[27] C. Kollath, A. Iucci, I. P. McCulloch, and T. Giamarchi, Phys. Rev. A **74**, 041604 (2006).
[28] I. Bloch, J. Dalibard, and W. Zwerger, Rev. Mod. Phys. **80**, 885 (2008).
[29] R. Jördens, N. Strohmaier, K. Günter, H. Moritz, and T. Esslinger, Nature (London) **455**, 204 (2008).
[30] R. Sensarma, D. Pekker, M. D. Lukin, and E. Demler, Phys. Rev. Lett. **103**, 035303 (2009).
[31] F. Massel, M. J. Leskinen, and P. Törmä, Phys. Rev. Lett. **103**, 066404 (2009).
[32] S. D. Huber and A. Rüegg, Phys. Rev. Lett. **102**, 065301 (2009).
[33] A. Korolyuk, F. Massel, and P. Törmä, Phys. Rev. Lett. **104**, 236402 (2010).
[34] N. Strohmaier, D. Greif, R. Jördens, L. Tarruell, H. Moritz, T. Esslinger, R. Sensarma, D. Pekker, E. Altman, and E. Demler, Phys. Rev. Lett. **104**, 080401 (2010).
[35] Z. Xu, S. Chiesa, S. Yang, S.-Q. Su, D. E. Sheehy, J. Moreno, R. T. Scalettar, and M. Jarrell, Phys. Rev. A **84**, 021607 (2011).
[36] D. Greif, L. Tarruell, T. Uehlinger, R. Jördens, and T. Esslinger, Phys. Rev. Lett. **106**, 145302 (2011).
[37] J. Heinze, S. Götze, J. S. Krauser, B. Hundt, N. Fläschner, D.-S. Lühmann, C. Becker, and K. Sengstock, Phys. Rev. Lett. **107**, 135303 (2011).
[38] A. Tokuno, E. Demler, and T. Giamarchi, Phys. Rev. A **85**, 053601 (2012).
[39] A. Tokuno and T. Giamarchi, Phys. Rev. A **85**, 061603 (2012).
[40] J. Heinze, J. S. Krauser, N. Fläschner, B. Hundt, S. Götze, A. P. Itin, L. Mathey, K. Sengstock, and C. Becker, Phys. Rev. Lett. **110**, 085302 (2013).
[41] A. Dirks, K. Mikelsons, H. R. Krishnamurthy, and J. K. Freericks, Phys. Rev. A **89**, 021602 (2014).
[42] P. Törmä and L. Tarruel in *Quantum Gas Experiments*, edited by P. Törmä and K. Sengstock (Imperial College Press, London, 2015), Chap. 10, p. 199.
[43] K. Loida, A. Sheikhan, and C. Kollath, Phys. Rev. A **92**, 043624 (2015).
[44] A. J. Daley, C. Kollath, U. Schollwöck, and G. Vidal, J. Stat. Mech. (2004) P04005.
[45] S. R. White and A. E. Feiguin, Phys. Rev. Lett. **93**, 076401 (2004).
[46] U. Schollwöck, Ann. Phys. (Amsterdam) **326**, 96 (2011).
[47] G. Delfino and G. Mussardo, Nucl. Phys. **B516**, 675 (1998).
[48] Z. Bajnok, L. Palla, G. Takács, and F. Wágner, Nucl. Phys. **B601**, 503 (2001).
[49] G. Takács and F. Wágner, Nucl. Phys. **B741**, 353 (2006).
[50] See Supplemental Material at http://link.aps.org/supplemental/10.1103/PhysRevLett.119.230403 for details on the time dependence of energy absorption, the absorption rate in the vicinity of Ising criticality and the bosonization calculations leading to the dynamic susceptibilities presented in the main text. This supplement includes Refs. [51–63].
[51] V. L. Berezinskii, Zh. Eksp. Teor. Fiz. **59**, 907 (1971) [Sov. Phys. JETP **32**, 493 (1971)].
[52] J. M. Kosterlitz and D. J. Thouless, J. Phys. C **6**, 1181 (1973).
[53] V. J. Emery in *Highly Conducting One-Dimensional Solids*, edited by J. T. Devreese, R. P. Evrard, and V. E. van Doren (Plenum Press, New York and London, 1979), p. 247.
[54] *Handbook of Mathematical Functions*, edited by M. Abramowitz and I. Stegun (Dover, New York, 1972).

[55] H. Bateman, *Higher Transcendental Functions*, edited by A. Erdelyi (McGraw-Hill, New York, 1953), Vol. 1.
[56] V. I. Smirnov, *A Course of Higher Mathematics* (Pergamon Press, New York, 1964), Vol. IV.
[57] M. Karowski and P. Wiesz, Nucl. Phys. **B139**, 455 (1978).
[58] F. A. Smirnov, *Form Factors in Completely Integrable Models of Quantum Field Theory* (World Scientific, Singapore, 1992).
[59] S. Lukyanov, Mod. Phys. Lett. A **12**, 2543 (1997).
[60] F. H. L. Essler and A. M. Tsvelik, Phys. Rev. B **57**, 10592 (1998).
[61] H. Babujian, A. Fring, M. Karowski, and A. Zapletal, Nucl. Phys. **B538**, 535 (1999).
[62] H. Babujian and M. Karowski, Nucl. Phys. **B620**, 407 (2002).
[63] F. H. L. Essler and R. M. Konik in *From Fields to Strings: Circumnavigating Theoretical Physics*, edited by M Shifman, A. Vainshtein, and J. Wheater (World Scientific, Singapore, 2012), p. 684.
[64] In contrast, the $n = 0$ peaks are expected at energies $\hbar\omega \sim (\pi\hbar u/4aL)$, which are too low in frequency to be resolved by our numerics.
[65] The sound velocities extracted from the other system sizes agree with this value within error bars.
[66] K. Loida, J.-S. Bernier, R. Citro, E. Orignac, and C. Kollath (to be published).
[67] P. Lecheminant, in *Frustrated Spin Systems*, edited by H. T. Diep (World Scientific, Singapore, 2005), Chap. 6, p. 307.
[68] L. W. Cheuk, M. A. Nichols, K. R. Lawrence, M. Okan, H. Zhang, E. Khatami, N. Trivedi, T. Paiva, M. Rigol, and M. W. Zwierlein, Science **353**, 1260 (2016).
[69] J. H. Drewes, L. A. Miller, E. Cocchi, C. F. Chan, N. Wurz, M. Gall, D. Pertot, F. Brennecke, and M. Köhl, Phys. Rev. Lett. **118**, 170401 (2017).
[70] A. Mazurenko, C. S. Chiu, G. Ji, M. F. Parsons, M. Kanász-Nagy, R. Schmidt, F. Grusdt, E. Demler, D. Greif, and M. Greiner, Nature (London) **545**, 462 (2017).
[71] A. L. Gaunt, T. F. Schmidutz, I. Gotlibovych, R. P. Smith, and Z. Hadzibabic, Phys. Rev. Lett. **110**, 200406 (2013).
[72] B. Mukherjee, Z. Yan, P. B. Patel, Z. Hadzibabic, T. Yefsah, J. Struck, and M. W. Zwierlein, Phys. Rev. Lett. **118**, 123401 (2017).
[73] K. Hueck, N. Luick, L. Sobirey, J. Siegel, T. Lompe, and H. Moritz, arXiv:1704.06315.